# Systematic pathway analysis using high-resolution fitness profiling of combinatorial gene deletions

Robert P St Onge[1], Ramamurthy Mani[2], Julia Oh[1], Michael Proctor[1], Eula Fung[1], Ronald W Davis[1], Corey Nislow[3], Frederick P Roth[2,4] & Guri Giaever[3]

Systematic genetic interaction studies have illuminated many cellular processes. Here we quantitatively examine genetic interactions among 26 *Saccharomyces cerevisiae* genes conferring resistance to the DNA-damaging agent methyl methanesulfonate (MMS), as determined by chemogenomic fitness profiling of pooled deletion strains. We constructed 650 double-deletion strains, corresponding to all pairings of these 26 deletions. The fitness of single- and double-deletion strains were measured in the presence and absence of MMS. Genetic interactions were defined by combining principles from both statistical and classical genetics. The resulting network predicts that the Mph1 helicase has a role in resolving homologous recombination–derived DNA intermediates that is similar to (but distinct from) that of the Sgs1 helicase. Our results emphasize the utility of small molecules and multifactorial deletion mutants in uncovering functional relationships and pathway order.

Complicating the relationship between genotype and phenotype is the fact that individual alleles sometimes combine to produce surprising phenotypes. The word 'epistasis' has been used in distinct ways, in both classical and statistical genetics, to describe this phenomenon[1]. Theoretical statistical-genetic arguments support the expectation that deleterious fitness effects of mutant alleles in independently functioning genes should combine multiplicatively; in other words, the double-mutant fitness is expected to be the product of the single-mutant fitness values[2]. The frequency with which this relationship occurs in nature is consequential to theories regarding evolution and the origins of sexual reproduction[3], but it remains unresolved after limited study[4–6]. Departure from the multiplicative model suggests that the corresponding gene products have a functional relationship, the nature of which depends on the 'direction' of the departure. Aggravating interactions, or 'negative epistasis' (in which the double-mutant fitness is lower than expected; synthetic lethality, in the extreme case), often reflect activities operating in separate but compensatory pathways[7]. Alleviating interactions, or 'positive epistasis' (in which the double-mutant fitness is greater than expected), often result when gene products operate in concert or in series within the same pathway. These interactions (also called 'diminishing-returns' interactions[2]) arise, for example, when a mutation in one gene impairs the function of a whole pathway, thereby concealing the consequence of additional mutations in other members of that pathway.

Several experimental studies and their analyses in *Saccharomyces cerevisiae* have illustrated the value of genome-scale screens for genetic interactions[8–20]. Screens for synthetic sick or lethal genetic interactions have uncovered numerous functional relationships, identified compensatory protein complexes and pathways, and offered insight into the nature of genetic robustness[8–17]. Most large-scale genetic interaction screens, however, have been restricted to the discovery of synthetic sick or lethal interactions and have defined such interactions by departure from the expectation that double-mutant strains will have the fitness of the least fit single mutant[8,10–12,14,15].
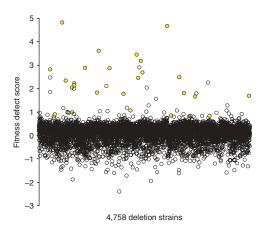
Although recent studies have expanded to include the measurement of alleviating interactions, these interactions have not been defined in a consistent way. In one case, a range of interaction types was defined by enumerating all possible 'greater than', 'less than' and 'equal to' relationships among single- and double-mutant invasive growth phenotypes[18]. In another case, epistasis was defined with the $S$-score[13], which identifies interactions from double mutants whose growth deviates from the median growth of all evaluated double mutants involving a given gene[20]. A theoretical study[19] defined interaction under the multiplicative neutral model[2] by using predicted growth rates, but ultimately favored an alternative measure ('scaled epsilon'). Neither of the latter two measures was evaluated experimentally.

Here we have conducted a comprehensive and quantitative analysis of genetic interactions among a target set of genes, focusing on non-essential genes that confer resistance to the DNA-damaging agent MMS. Quantitative fitness analysis identified both aggravating and alleviating interactions on the basis of deviation from a multiplicative model. Because of the quantitative nature of our assay, we

[1]Department of Biochemistry, Stanford University, Stanford, California 94305, USA. [2]Biological Chemistry and Molecular Pharmacology Department, Harvard, Boston, Massachusetts 02115, USA. [3]Department of Pharmaceutical Sciences, Leslie Dan Faculty of Pharmacy, Donnelly Centre for Cellular and Biomolecular Research, University of Toronto, Toronto, Ontario M5S3E1, Canada. [4]Center for Cancer Systems Biology, Dana-Farber Cancer Institute, 44 Binney Street, Boston, Massachusetts 02115, USA. Correspondence should be addressed to F.P.R. (froth@hms.harvard.edu) or G.G. (guri.giaever@utoronto.ca).

**Figure 1** Identification of genes that confer resistance to MMS. Chemogenomic profiling of the homozygous diploid (BY4743) collection of deletion mutants with MMS. Fitness defect scores, based on barcode microarray hybridization and calculated as described[21], are plotted on the y axis for 4,758 deletion strains arranged alphabetically across the x axis. Twenty-six deletion strains that were analyzed further are highlighted in yellow. MMS-sensitive strains showing severe growth defects in the absence of MMS, or corresponding to deletions that overlapped other genes in the selected set, were not pursued further.

could also differentiate among 'classical genetic' subclasses of alleviating interactions on the basis of the relative MMS sensitivity of single- and double-deletion strains. We used a systematic, objective and automated analysis of the genetic evidence to derive an interaction network that recapitulates many known features of DNA repair pathways. This interaction network also makes predictions, including a role for the Mph1 helicase in resolving DNA intermediates resulting from homologous recombination.

## RESULTS

### Selection, construction and fitness of double-deletion mutants

We systematically assessed genetic interactions among a target subset of genes that confer resistance to the compound MMS. These genes were selected on the basis of the results of a chemogenomic fitness screen of pooled homozygous yeast deletion strains[21,22] (**Fig. 1** and **Supplementary Table 1** online). Deletion strains that were among the most sensitive to MMS (**Fig. 1**) were used to construct all possible combinations of double-deletion strains for quantitative fitness analysis (see Methods). To facilitate construction of these mutants, each gene was deleted in haploid strains of both mating types. In MATa haploids (BY4741), genes were replaced with a gene encoding the kanamycin resistance marker gene (Kan[r]). In the MATα haploid strain (Y5563), genes were replaced with a gene encoding the nourseothricin

resistance marker gene (Nat[r]). Y5563 contains the *can1Δ::MFApr-HIS3* marker necessary for the selection of double-deletion haploid mutants[14]. The doubling time (D) of all single-deletion strains in rich growth medium (YPD) with and without 0.002% MMS was measured by using a highly quantitative growth assay (Methods and **Fig. 2a**). Deletion strains for which the doubling time of the Kan[r] strain was inconsistent with that of the Nat[r] strain were either reconstructed and verified to eliminate inconsistencies or omitted from further analysis (data not shown).

The doubling times of single mutants (with and without MMS) ranged from 1.3 h to 8 h, and the average coefficient of variation (CV), calculated from not fewer than five replicates, was 5.2%. Only a modest increase in CV was observed for strains with the most severe growth defects (**Supplementary Fig. 1** online). This method provided the sensitivity and precision necessary for distinguishing small differences in growth rate, which were essential for our subsequent analysis (**Supplementary Fig. 1**). The fitness of each deletion strain was defined by its growth rate relative to that of wild type (calculated as the doubling time of the parental wild-type strain divided by that of the mutant). The average fitness values of single-deletion strains used for further analysis are shown in **Figure 2b**. Notably, all 26 gene deletions resulted in reduced fitness relative to the wild-type control.

We used the 26 Kan[r] haploid deletion strains and 26 Nat[r] haploid deletion strains to construct 650 double-deletion strains. Four of these strains could not be constructed because of genetic linkage between genes. Ten other strains were nonviable (synthetically lethal) and were assigned a fitness of zero. The fitness of the remaining 636 double-deletion strains was measured in YPD media both with and without MMS (see Methods). A benefit of this approach is that
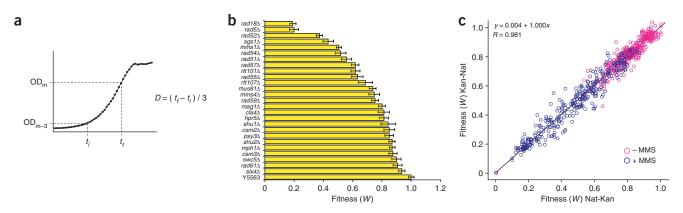


**Figure 2** Fitness measurement of single- and double-deletion strains. (**a**) Calculation of the doubling time (D) of individual deletion strains during exponential growth. D is the difference between the time $t_f$ at an arbitrary maximum OD (OD$_m$) and the time $t_i$ at a point three generations earlier (OD$_{m-3}$), divided by the number of generations (D = ($t_f − t_i$)/3). (**b**) Mean fitness of 26 single-deletion strains in 0.002% MMS. Fitness (W) for a strain with gene x deleted was calculated by dividing the average D of wild type (Y5563) by that of the deletion strain (W = $D_{wt}/D_{yfgΔ}$). Fitness values were averaged from MATa Kan[r] (BY4741) and MATα Nat[r] (BY4742) deletion strains; error bars represent the s.d. from no fewer than seven replicate measurements. (**c**) Fitness correlation between reciprocal double-deletion mutants for each unique gene pair in the presence and absence of MMS. The fitness of Kan[r]-Nat[r] double-deletion strains is plotted on the y axis and the Nat[r]-Kan[r] fitness is plotted on the x axis. The correlation coefficient (R) and best-fitting line are shown.

each gene pair is represented by two independently constructed double-deletion strains (referred to as the 'Kan$^r$-Nat$^r$' and 'Nat$^r$-Kan$^r$' strains). To quantify the robustness of our strain construction and fitness assay, we plotted the fitness (calculated in both the presence and the absence of MMS) of the Kan$^r$-Nat$^r$ double-deletion strains against that of the Nat$^r$-Kan$^r$ deletion strains (**Fig. 2c**). We obtained a highly significant correlation ($R = 0.981$) with a slope near to 1, consistent with the idea that strain construction contributed negligibly to fitness.

### Quantitative genetic interactions predict shared function

If the deleterious effects of two distinct mutations are truly independent of one another, then their fitness defects are predicted to combine multiplicatively[2]. In other words, if a strain deleted for gene $x$ has a fitness $W_x$ and a strain deleted for gene $y$ has a fitness $W_y$, then the fitness of the double mutant strain $W_{xy}$ is expected to be $W_x \times W_y$. Using the double- and single-deletion fitness values calculated in **Figure 2**, we measured the deviation $\varepsilon$ from this expectation (where $\varepsilon_{xy} = W_{xy} - W_x \times W_y$) and found that $\varepsilon$ values were highly correlated between reciprocal double-deletion pairs ($R = 0.896$; data not shown). The $\varepsilon$ values derived from averaging the fitness of the Kan$^r$-Nat$^r$ and Nat$^r$-Kan$^r$ mutants are given in **Supplementary Table 2** online and are represented as a heat map in **Figure 3a**.

Given that deviation from neutrality (nonzero $\varepsilon$) suggests a functional relationship, we assessed how well current knowledge of these genes was reflected in the $\varepsilon$ values. We examined the distribution of $\varepsilon$ value for gene pairs with or without a specific functional link—in other words, gene pairs that either do or do not share a specific gene ontology (GO) term[23]. Whereas the distribution of $\varepsilon$ values for genes without a specific functional link is centered near zero, the $\varepsilon$ values of the 35 functionally linked gene pairs are clearly centered away from zero and are predominantly positive (**Fig. 3b**).

Prediction of specific functional linkage on the basis of the $\varepsilon$ value alone achieved a sensitivity of 80% at a false-positive rate of 20% (**Fig. 3c**), as assessed by cross-validation. Hierarchical clustering of genes by genetic congruence (that is, correlation of $\varepsilon$ profiles[15,24]; see Methods) showed that the similarity between the spectrum of genetic interactions of two genes was also a robust predictor of functional links (**Fig. 3c**). This is consistent with the observation that genetic congruence can predict shared function[15,24]. We found that a combination of $\varepsilon$, genetic congruence, and a measure of the difference between the MMS sensitivity of the double mutant and each single mutant (described in more detail below) was the most robust predictor of specific functional links. Using the combined predictor, we achieve a sensitivity of 84% at a false-positive rate of 20%. Moreover, at a lower false-positive rate of 2%, the combined predictor achieves 54% sensitivity, as compared with 20% achieved with $\varepsilon$ alone
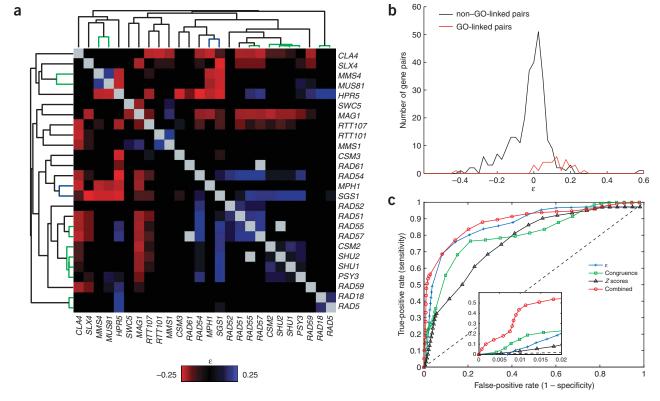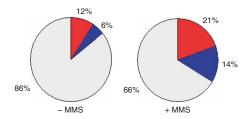


**Figure 3** Quantitative genetic interactions predict shared function. (**a**) Genes clustered according to similar patterns of deviation ($\varepsilon$) of double-deletion fitness ($W_{xy}$) from the expectation for non-interacting loci ($W_x \times W_y$). Fitness values were obtained from growth in the presence of 0.002% MMS. Hierarchical clustering of genes was performed on the basis of genetic congruence (Pearson correlation of $\varepsilon$ profiles). (**b**) Distribution of $\varepsilon$ values for all gene pairs grown in the presence of MMS (bin size 0.025). Gene pairs with specific functional links are in red (GO-linked pairs); gene pairs not sharing specific functional links are in black (non-GO–linked pairs). (**c**) Comparison of the ability to predict functional links of $\varepsilon$ values, genetic congruence of $\varepsilon$ profiles, and Z-scores assessing the proximity of the MMS sensitivity of double-deletion strains to the sensitivity of single-deletion strains. The combination of each of these is also assessed ('Combined'). For each predictor, the true-positive rate or 'sensitivity' (defined here as the fraction of gene pairs correctly predicted to have functional links) and false-positive rate or '1 − specificity' (defined here as the fraction of non-functionally linked gene pairs incorrectly predicted to have functional links) are shown at a series of score thresholds.

**Figure 4** Identification of significant genetic interactions. Significant departure ($P < 0.01$) from a multiplicative model in which $W_{xy} = W_x \times W_y$ is used to define aggravating and alleviating genetic interactions. The percentage of aggravating (red), alleviating (blue) and neutral (gray) gene pairs identified are compared in the presence and absence of MMS.

(**Fig. 3c**). We also note that 'scaled epsilon', a previously proposed measure of genetic interaction[19], was not as effective at predicting functional links (**Supplementary Fig. 2** online).

### Identification of significant genetic interactions

Because two gene pairs with the same ε value may have different susceptibilities to measurement error, we used a $Z$-test based on estimated errors in fitness measurements of single- and double-deletion strains to detect significant departure ($P < 0.01$) of each gene pair from the multiplicative model (see Methods). We applied this method to fitness measurements obtained both with and without MMS, and found that the addition of MMS increased the number of both aggravating and alleviating interactions (**Fig. 4**). In the presence

of MMS, 113 out of 323 pairs were found to deviate significantly from the multiplicative model. Of these, 45 were classified as alleviating interactions (significantly positive ε) and 68 were classified as aggravating interactions (significantly negative ε). Classification results for all 323 gene pairs are given in **Supplementary Table 2**.

Of the 45 gene pairs with significantly positive ε (see below), 24 had a functional link. Of the 21 alleviating interactions that did not have a functional link, many have well-documented interactions including *MUS81-MMS4* (ref. 25), *SGS1-SHU1*, *SGS1-SHU2* and *SGS1-PSY3* (ref. 26); *HPR5-RAD18* and *HPR5-RAD5* (ref. 27); *RAD5-RAD18* (ref. 28); and *SHU1-SHU2* (ref. 29). Most gene pairs in our data set were classified as neutral, even when cells were grown in the presence of MMS. The limited connectivity of alleviating interactions was marked given that the genes studied were already enriched for a common function (conferring resistance to MMS). This observation suggests that the functional information provided by alleviating interactions is specific rather than general.

### Subclassification of alleviating interactions

We focused further on the 45 gene pairs classified as alleviating in MMS, dividing them into five distinct categories based on the relative MMS sensitivity ($S$; see Methods) of single- and double-deletion strains (**Fig. 5a**). Restricting these analyses to MMS-induced growth defects enabled us to focus on pathways responding specifically to MMS-induced lesions, which was important because approximately half of the deletion strains studied showed fitness defects even in the absence of MMS (data not shown). Fourteen pairs showed 'masking epistasis' ($S_{xy} = S_x > S_y$), whereas four showed partial
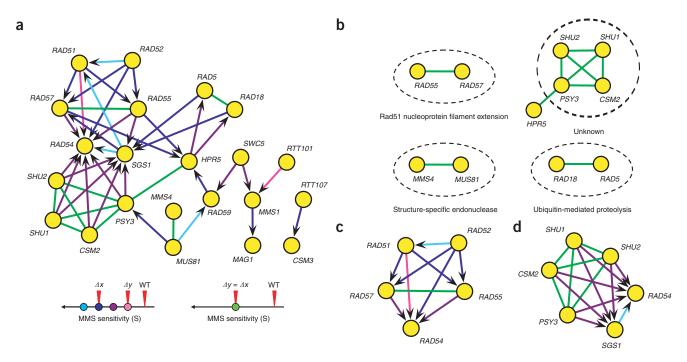


**Figure 5** Subclassification of alleviating interactions. (**a**) Subclassification of 45 alleviating interactions on the basis of similarity of MMS sensitivity ($S = D_{+MMS}/D_{−MMS}$) of each double-deletion strain ($S_{xy}$) to its corresponding single-deletion strains ($S_x$ and $S_y$), as measured by $Z$-scores (see Methods). Genes are represented by nodes. Arrows represent five alleviating interaction subtypes: coequal (green), partial masking (light blue), masking (dark blue), partial suppression (purple), suppression (pink). These interaction types are shown below (red arrowheads indicate single-deletion MMS sensitivities; colored circles represent double-deletion sensitivities). (**b**) Ten coequal interactions identify functionally cohesive units. Nine correspond to known or predicted protein interactions, as indicated by the broken circles. (**c**) Asymmetric alleviating interactions ($S_x > S_y$) between core members of the homologous recombination pathway (*RAD51*, *RAD52*, *RAD54*, *RAD55* and *RAD57*). For masking interactions (both partial and complete), arrows are drawn from the masking locus ($x$); for suppressing interactions (both partial and complete), arrows are drawn from the suppressing locus ($y$). (**d**) Partial suppression of the MMS sensitivities of *sgs1Δ* and *rad54Δ* by deletions in Shu complex genes (*SHU1*, *SHU2*, *CSM2* and *PSY3*).

masking epistasis ($S_{xy} > S_x > S_y$). This scenario may be intuitively viewed as the deletion in gene $x$ 'masking' the effects of the deletion in gene $y$. In addition, 2 gene pairs showed complete suppression ($S_{xy} = S_y < S_x$) and 15 showed partial suppression ($S_y < S_{xy} < S_x$). In this scenario the deletion in gene $y$ improves the phenotype associated with the gene $x$ deletion. Lastly, we observed ten gene pairs for which the MMS sensitivity of the single- and double-deletion strains was statistically indistinguishable ($S_{xy} = S_x = S_y$). These interactions, which we call 'coequal', are related to 'complementary gene action', 'complementary epistasis' or 'asynthetic' relationship types that have been previously described[18,30,31].

Coequal relationships suggest that the genes function as cohesive units. For example, if two genes encode distinct subunits of a given protein complex, then we would expect these genes to show a coequal relationship (if neither gene has an additional function and if the protein complex requires both subunits for its function). Nine of the ten coequal interactions that we detected (all but *PSY3-HPR5*) encode, or are predicted to encode, physically interacting proteins[25,26,28,32,33] (**Fig. 5b**). This suggests that disruption of each gene alone is sufficient to disrupt the function of the protein complex to which it contributes, and that neither gene has a separate function under the conditions examined. Apart from the *PSY3-HPR5* pair, the coequal interacting pairs tended to have the highest congruence scores (**Fig. 3a**).

Asymmetric alleviating interactions (where $S_x \neq S_y$) can be used to infer the order of biochemical events in a pathway[34]. For example, the phenotype of an $x\Delta y\Delta$ mutant resembling that of $x\Delta$, but not $y\Delta$, could be explained by protein X operating upstream of protein Y in a pathway (under the positive regulatory model of Avery and Wasserman[34]). We found that the genetic interactions among five genes central to homologous recombination (*RAD51*, *RAD52*, *RAD54*, *RAD55* and *RAD57*; hereafter termed 'homologous recombination genes') can recapitulate the current model for the biochemical steps carried out by their encoded proteins (**Fig. 5c**). The first step of this process involves recruitment of the Rad51 protein to single-stranded DNA by Rad52. Extension of the resulting Rad51-nucleoprotein filament is then mediated by the Rad55-Rad57 heterodimer. Sub-sequent strand displacement at a region of homology is mediated by interactions with Rad54 (reviewed in ref. 35). This order is also consistent with the genetic dependencies for relocalization of these proteins to sites of DNA damage[36].

The most highly connected module of alleviating interactions involved four genes (*SHU1*, *SHU2*, *CSM2* and *PSY3*) that encode members of a protein complex collectively referred to hereafter as the 'Shu complex'. Notably, we found coequal interactions between all pairs of Shu complex genes. Consistent with a previous report, deletions in each of these four genes partially suppressed the MMS sensitivity of the *sgs1Δ* strain[26]. We found that these four deletions also partially suppressed the *rad54Δ* deletion phenotype (**Fig. 5d**) and rescued the synthetic lethality between *rad54Δ* and *hpr5Δ* (**Supplementary Fig. 3** online). These results extend previous findings supporting the idea that the Shu complex has a role in homologous recombination[26] and place it upstream of Rad54.

**Predicted role of Mph1 in resolving DNA repair intermediates**

*SGS1* encodes a highly conserved member of the bacterial RecQ helicase family and shares homology with human *BLM*, which has mutations associated with Bloom's syndrome[37]. Sgs1 has been proposed to function closely with the homologous recombination machinery. The synthetic lethality of *sgs1Δmus81Δ* and *sgs1Δmms4Δ* double-deletion strains can be rescued by eliminating early steps in homologous recombination (for example, the triple mutant *sgs1Δmms4Δrad51Δ* is viable[38]). This observation has led to the hypothesis that the helicase activity of Sgs1 and the endonuclease activity of the Mus81-Mms4 complex[25] are each important for resolving a common cytotoxic homologous recombination-generated DNA intermediate[38]. Consistent with this hypothesis, recombination-dependent cruciform structures have been found to accumulate in *sgs1Δ* cells and to be actively resolved when *SGS1* is overexpressed[39].

Hierarchical clustering of ε values showed that the *sgs1Δ* strain and the *mph1Δ* strain share a similar pattern of ε values (**Fig. 3a**). This similarity, which includes aggravating interactions with both *mus81Δ*
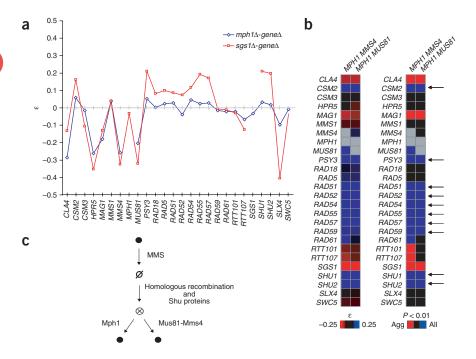


**Figure 6** Predicted role of Mph1 in resolving homologous recombination–generated DNA intermediates. (**a**) Line graph emphasizing the similarity in ε profiles of *sgs1Δ* (red) and *mph1Δ* (blue). Deviation from multiplicative expectation (ε) is plotted on the y axis and genes are arranged alphabetically on the x axis. (**b**) Heat map representing the effect of 26 gene deletions (vertical axis) on the fitness of *mph1Δmms4Δ* and *mph1Δmus81Δ* double-deletion strains (horizontal axis). Raw ε values (where $\varepsilon = W_{xyz} - W_{xy} \times W_z$) are shown on the left; significant deviations ($P < 0.01$) from expectation are represented on the right. Ten genes found to be consistently alleviating (arrows) were analyzed further (**Supplementary Fig. 5**). (**c**) Model of the potential role of MPH1 in resolving homologous recombination-dependent DNA intermediates (●, undamaged DNA; ∅, MMS-damaged DNA; ⊗, toxic DNA intermediates).

and *mms4Δ*, is emphasized in **Figure 6a**. Mph1, similar to Sgs1, possesses 3′ to 5′ helicase activity[40], shows alleviating interactions with components of homologous recombination[41], and has a human ortholog implicated in a disorder associated with genomic instability[42]. We therefore tested whether the aggravating phenotype of *mph1Δmus81Δ* and *mph1Δmms4Δ* double-deletion strains could be suppressed by mutations in homologous recombination–associated or other genes in our data set. Triple-deletion strains were created by crossing both the 'Kan$^r$-Nat$^r$' and 'Nat$^r$-Kan$^r$' variants of *mph1Δmus81Δ* and *mph1Δmms4Δ* double-deletion strains to each of the remaining 24 MATα haploids in which genes were replaced with a *hygB$^r$* selectable marker (see Methods). The fitness of each triple-deletion strain was then measured in the presence of MMS.

The expected fitness deviated from expectation for several triple-deletion strains, and the sign of the observed deviation tended to be same in the *mph1Δmms4Δ* and *mph1Δmus81Δ* backgrounds (**Fig. 6b**). Of the 24 gene deletions, 10 were found to show alleviating interactions on both backgrounds. These ten genes are the core factors in homologous recombination (*RAD51*, *RAD52*, *RAD54*, *RAD55* and *RAD57*), members of the Shu complex (*SHU1*, *SHU2*, *CSM2* and *PSY3*) and *RAD59*, a homolog of *RAD52* that functions in a Rad51-independent homologous recombination pathway[43]. In addition, all ten deletions (apart from *rad52Δ*) improved the fitness of both of the *mph1Δmus81Δ* and the *mph1Δmms4Δ* double-deletion strains in the presence of MMS (data not shown and **Supplementary Fig. 4** online). Consistent with previous reports, each of these deletions (with the notable exception of *rad59Δ*) rescued the synthetic lethality of both *sgs1Δmus81Δ* and *sgs1Δmms4Δ* (ref. 38 and **Supplementary Fig. 5** online). Collectively, these results suggest that Mph1 has a role in resolving homologous recombination–dependent and Shu complex–dependent toxic DNA intermediates (**Fig. 6c**).

Our analysis of double mutants did not identify previously reported interactions between *MPH1* and homologous recombination genes[41], between *MPH1* and Shu complex genes[21], or between homologous recombination genes and Shu complex genes[26]. Even though the ε values for these pairs were consistently positive (**Fig. 6a** and **Supplementary Table 2**), significant deviation from the multiplicative model was rarely observed. When we aggregated the ε scores for the four Shu complex genes, we detected significant positive deviation from expectation between this complex and both *MPH1* and the homologous recombination genes; however, these deviations were significantly weaker than those measured for pairs of Shu complex genes (**Supplementary Fig. 6** online). These differences in ε magnitude cannot be explained by variations in single-deletion fitness defects. Thus, although our results are consistent with the idea that Mph1, homologous recombination proteins and the Shu complex operate in a common pathway, they suggest that Mph1, homologous recombination proteins and the Shu complex also have cellular roles that are independent of one another. Capturing such partially overlapping relationships in future systematic studies of alleviating interactions will prove challenging.

### DISCUSSION

We have described a comprehensive and quantitative analysis of genetic interactions among 26 non-essential genes involved in resistance to MMS-induced DNA damage. A conceptually simple multiplicative model was used to define genetic interactions between these genes. The validity of this model is supported here by the fact that the fitness defects of gene pairs without functional links usually combine multiplicatively, and that deviation from this model is predictive of shared function. This model has not been applied in previous large-scale genetic interaction studies[8,10–12,14,15,18]. As a result, some gene pairs might have been previously misinterpreted as being in common or compensatory pathways if the multiplicative neutral model adopted here is correct.

In the absence of MMS, our methods classified 12% of gene pairs as aggravating interactions and 6% as alleviating interactions (**Fig. 4**). Genome-wide screens have estimated the frequency of aggravating genetic interactions (synthetic lethality and synthetic sickness) to be ∼0.5% among non-essential genes[15]. The ∼24-fold enrichment in aggravating interaction frequency that we observed in the absence of MMS illustrates the utility of chemogenomic fitness screens in identifying functionally related subsets of genes and in quantitatively measuring their genetic interactions. Notably, we further enriched the number of alleviating and aggravating interactions to 21% and 14%, respectively, by growing deletion strains in the presence of MMS. The enrichment of functional links among alleviating gene pairs further underscores the value of systematic screens that can capture such interactions[13,18].

The adaptive value of the sexual mode of reproduction has been much debated. The deterministic theory argues that, if aggravating epistasis is prevalent, then sexual reproduction is selective because it enables deleterious mutations to be purged from genomes[3]. Previous studies aimed at measuring the relative frequencies of alleviating and aggravating interactions have yielded conflicting results[4–6]. Here, all single-gene deletions produced a quantifiable phenotype relative to wild type (**Fig. 1b**); thus, every gene pair in our data set was interrogated for both alleviating and aggravating interactions. The observation that aggravating interactions occurred more frequently than alleviating interactions (**Fig. 4**; both with and without MMS) is consistent with the deterministic theory. An important caveat, however, is that the genes that we studied were not chosen randomly.

The relative MMS sensitivities of single and double mutants were used to distinguish distinct subtypes of alleviating genetic interactions. We found that coequal interactions (where $S_{xy} = S_x = S_y$) occur between gene pairs that typically have the highest genetic congruence scores (**Figs. 3a** and **5b**) and coequality is generally indicative of protein complexes that function as cohesive units[25,26,28,32,33]. Systematically discovered alleviating interactions (where $S_x \neq S_y$) accurately predicted the order of previously characterized biochemical processes. In addition, we found that *shu1Δ*, *shu2Δ*, *psy3Δ* and *csm2Δ* could partially suppress the MMS sensitivity of *rad54* (**Fig. 5b**) and, similar to deletions in homologous recombination genes[44], rescue the synthetic lethality of an *hpr5Δrad54Δ* double-deletion mutant (**Supplementary Fig. 3**). These data extend previous findings linking the Shu complex to homologous recombination[26] and place this complex upstream of Rad54 in homologous recombination–mediated repair of both MMS-induced and spontaneous DNA damage.

Genetic congruence between *MPH1* and *SGS1* led to the hypothesis and observation that the fitness of *mph1Δmus81Δ* and *mph1Δmms4Δ* double-deletion strains in MMS can be improved by deleting genes important for homologous recombination and is consistent with the idea that the Mph1 helicase is involved in resolving homologous recombination-dependent toxic DNA intermediates (**Fig. 6**). Even though the Mph1 protein shows similar substrate specificity to Sgs1 *in vitro*[40], whether it has the same substrate specificity as Sgs1 *in vivo* remains to be determined. Two of our results argue against this possibility: first, we did not observe any interaction between these two genes, as might be expected if they resolve the same intermediate; and second, although the *rad59Δ* deletion suppressed the sensitivity of *mph1Δmus81Δ* and *mph1Δmms4Δ*, it did not rescue the synthetic lethality of *sgs1Δmus81Δ* or *sgs1Δmms4Δ*. This observation suggests

that Mph1 may distinguish itself from Sgs1 by acting on substrates generated by a *RAD59*-dependent mechanism[45].

Of the roughly 6,000 genes in the yeast genome, fewer than 1,200 are essential for viability under optimal growth conditions (rich medium at 30 °C)[22,46]. Consistent with studies involving random mutations[4,5] and computational studies of yeast metabolism[19], most of our gene pairs followed a multiplicative relationship (**Fig. 4**). This level of robustness will undoubtedly hinder efforts to understand the functional organization of the cell on a systems level. Our results emphasize the utility of systematic and quantitative double-deletion studies, but they also show that additional perturbations, either genetic or chemical, will be necessary to reveal the full architecture of cellular pathways.

## METHODS

**Strains and media.** All strains were maintained on YPD media[47,48]. Antibiotic-resistant strains were selected with 200 μg/ml of genetecin (Agri-Bio), 100 μg/ml of nourseothricin (Werner Bioagents) and/or 300 μg/ml of hygromycin B (Agri-Bio). Single-deletion strains were obtained from the yeast deletion collection or were constructed *de novo* by PCR-based gene replacement[49]. Double-deletion strains were constructed by the synthetic genetic array (SGA) protocol[14] with minor modifications. Cells were transferred manually with a 96-head pin tool and subjected to three rounds of selection before being pinned onto YPD/agar plates, grown for 2 d, and stored at 4 °C. Triple-deletion strains were constructed essentially as above, by crossing single-deletion HygB[r] MATα haploids to double-deletion Kan[r]-Nat[r] MATa haploids and by selecting sporulated diploids on double-deletion selection media supplemented with hygromycin B.

Double- and triple-deletion strains were reconstructed by sporulating diploid heterozygotes and dissecting tetrads, or by selecting random spores if they met one of the following three criteria: (i) a viable colony was not obtained, (ii) the strain fitness was found to be higher than that of both starting strains ($W_{xy} - \max(W_x, W_y) > 0.05$), or (iii) the fitness of Kan[r]-Nat[r] double-deletion strains differed from that of the Nat[r]-Kan[r] deletion strains ($|W_{xy} - W_{yx}|/\sqrt{2} > 0.15$). *rad57Δrad61Δ* and *rad55Δshu2Δ* double-deletion strains were not constructed because of genetic linkage between their respective gene pairs. Ten double-deletion mutants involving five confirmed synthetic lethal pairs (*sgs1Δmus81Δ*, *sgs1Δmms4Δ*, *sgs1Δslx4Δ*, *rad54Δhpr5Δ* and *sgs1Δhpr5Δ*) were assigned a fitness of zero.

**Growth assay.** Individual deletion strains arrayed on YPD/agar were inoculated into 80 μl of YPD using a 96-head pin tool. Cultures were grown to saturation for 20 h at 30 °C and then stored at 4 °C for 4–48 h. The cells were then resuspended by shaking for 15 min, and the optical density at 600 nm (OD$_{600}$) of cultures was determined using a Tecan GENios microplate reader (Tecan). Cell concentrations were normalized by diluting each culture to a final OD$_{600}$ of 0.02 with YPD using a Biomek FX Laboratory Automation Workstation (Beckman Coulter). Normalized cultures were grown in 100-μl volumes in 96-well plates in Tecan GENios microplate readers for 24 h. The growth rate of each culture was monitored by measuring the OD$_{600}$ every 15 min.

The doubling time ($D$) was calculated from the difference between the time $t_f$ at an arbitrary maximum OD$_{600}$ (OD$_m$) and the time $t_i$ at a point three generations earlier, divided by the number of generations: $D = (t_f - t_i)/3$. The OD$_m$ is usually in the exponential growth regime and is approximately the OD$_{600}$ after five doublings from the beginning of the run. OD$_m$ is divided iteratively by 2 to calculate the OD$_{m-3}$ point at three generations earlier. For growth curves that do not reach saturation or OD$_m$ during the growth run, OD$_m$ is reassigned to the maximum OD$_{600}$ of the curve. The fitness ($W$) of a strain deleted for a given gene $x$ was defined as the ratio of the doubling time ($D$) of the wild-type strain to the deletion strain ($W = D_{wt}/D_x$).

**Classification of genetic interactions.** Genetic interaction between a pair of genes ($x,y$) was defined if the fitness phenotype of the double mutant ($W_{xy}$) deviated significantly from that predicted for non-interacting gene pairs ($W_x \times W_y$) under the multiplicative model. For each gene pair, the test used estimates of the mean and s.d. of $W_{xy}$ derived by treating Kan[r]-Nat[r] and Nat[r]-Kan[r] strains

as replicates. In addition, the delta method was used to compute the mean and s.d. of the product $W_x \times W_y$ on the basis of the means and s.d. of $W_x$ and $W_y$ obtained with the replicates in the single-deletion growth analysis. Gene pairs for which the multiplicative model hypothesis could be rejected ($Z$-test, α = 0.01) were categorized as genetic interactions. Interacting pairs were further classified as aggravating or alleviating depending on whether the double-deletion fitness phenotype was lesser or greater, respectively, than the product of the single-deletion fitness measurements.

**Subclassification of alleviating interactions.** Alleviating interactions were subdivided into five unique categories depending on their MMS sensitivity $S$, where $S = D_{+MMS}/D_{-MMS}$. $Z$-scores were used to measure the proximity of the MMS sensitivity of a double mutant to the sensitivities of the corresponding single mutants, $x$ and $y$, with the respective formulae:

$$(\mu_{Sxy} - \mu_{Sx})/\sqrt{\sigma_{Sxy}^2 + \sigma_{Sx}^2}$$

and

$$(\mu_{Sxy} - \mu_{Sy})/\sqrt{\sigma_{Sxy}^2 + \sigma_{Sy}^2}$$

where μ and σ represent, respectively, the mean and estimated error of replicate measures of the variable indicated in the subscript. $Z$-scores under 0.75 were judged to be roughly equal for the purposes of subclassifying alleviating interactions. Directionality was assigned to asymmetric alleviating interactions (where $S_x > S_y$) as follows: for masking interactions (both partial and complete), network arrows originate from the masking locus ($x$); for suppressing interactions (both partial and complete), network arrows originate from the suppressing locus ($y$).

**Prediction of shared function.** Gene ontology (GO) links ('specific functional links') were assigned to each gene pair with a specific biological process GO term in common. A GO term was considered to be specific if it is associated with fewer than 30 genes. To assess the value of quantitative genetic interactions in predicting functional links, we used several predictors: ε, genetic congruence (Pearson correlation between ε profiles, calculation for genes $x$ and $y$ excluding $\varepsilon_{xy}$, and undefined $\varepsilon_{xx}$ and $\varepsilon_{yy}$ values), and $Z$-scores measuring proximity of the double-deletion MMS sensitivity to the nearest single-deletion MMS sensitivity. The final model combined all of these predictors through a single logistic regression scheme. Regression equations were calculated by using the *glmfit* and *glmval* functions in MATLAB (MathWorks). Each model was assessed for its ability to predict functional links by using sixfold cross-validation. The prediction sensitivity or true-positive rate (defined here as the fraction of functionally linked gene pairs correctly predicted to have functional links) and false-positive rate (defined here as the fraction of non-functionally linked gene pairs incorrectly predicted to have functional links) are measured at a series of score thresholds (**Fig. 3c**).

**Accession numbers.** The Swiss-Prot accession numbers for the single-deletion strains are as follows: *CLA4* (P48562), *CSM2* (P40465), *CSM3* (Q04659), *HPR5* (P12954), *MAG1* (P22134), *MMS1* (Q06211), *MMS4* (P38257), *MPH1* (P40562), *MUS81* (Q04149), *PSY3* (Q12318), *RAD5* (P32849), *RAD18* (P10862), *RAD51* (P25454), *RAD52* (P06778), *RAD54* (P32863), *RAD55* (P38953), *RAD57* (P25301), *RAD59* (Q12223), *RAD61* (Q99359), *RTT101* (P47050), *RTT107* (P38850), *SGS1* (P35187), *SHU1* (P38751), *SHU2* (P38957), *SLX4* (Q12098) and *SWC5* (P38326).

**URLs.** Swiss-Prot: http://www.ebi.ac.uk/swissprot

*Note: Supplementary information is available on the Nature Genetics website.*

1. Phillips, P.C. The language of gene interaction. *Genetics* **149**, 1167–1171 (1998).
2. Phillips, P.C., Otto, S.P. & Whitlock, M.C. *Beyond the Average: the Evolutionary Importance of Gene Interactions and Variability of Epistatic Effects in Epistasis and the Evolutionary Process* 20–38 (Oxford Univ. Press, New York, 2000).
3. Kondrashov, A.S. Deleterious mutations and the evolution of sexual reproduction. *Nature* **336**, 435–440 (1988).
4. Szafraniec, K., Wloch, D.M., Sliwa, P., Borts, R.H. & Korona, R. Small fitness effects and weak genetic interactions between deleterious mutations in heterozygous loci of the yeast *Saccharomyces cerevisiae*. *Genet. Res.* **82**, 19–31 (2003).
5. Elena, S.F. & Lenski, R.E. Test of synergistic interactions among deleterious mutations in bacteria. *Nature* **390**, 395–398 (1997).
6. Maisnier-Patin, S. *et al.* Genomic buffering mitigates the effects of deleterious mutations in bacteria. *Nat. Genet.* **37**, 1376–1379 (2005).
7. Hartman, J.L., IV, Garvik, B. & Hartwell, L. Principles for the buffering of genetic variation. *Science* **291**, 1001–1004 (2001).
8. Davierwala, A.P. *et al.* The synthetic genetic interaction spectrum of essential genes. *Nat. Genet.* **37**, 1147–1152 (2005).
9. Kelley, R. & Ideker, T. Systematic interpretation of genetic interactions using protein networks. *Nat. Biotechnol.* **23**, 561–566 (2005).
10. Ooi, S.L. *et al.* Global synthetic-lethality analysis and yeast functional profiling. *Trends Genet.* **22**, 56–63 (2006).
11. Ooi, S.L., Shoemaker, D.D. & Boeke, J.D. DNA helicase gene interaction network defined using synthetic lethality analyzed by microarray. *Nat. Genet.* **35**, 277–286 (2003).
12. Pan, X. *et al.* A DNA Integrity network in the yeast *Saccharomyces cerevisiae*. *Cell* **124**, 1069–1081 (2006).
13. Schuldiner, M. *et al.* Exploration of the function and organization of the yeast early secretory pathway through an epistatic miniarray profile. *Cell* **123**, 507–519 (2005).
14. Tong, A.H. *et al.* Systematic genetic analysis with ordered arrays of yeast deletion mutants. *Science* **294**, 2364–2368 (2001).
15. Tong, A.H. *et al.* Global mapping of the yeast genetic interaction network. *Science* **303**, 808–813 (2004).
16. Wong, S.L., Zhang, L.V. & Roth, F.P. Discovering functional relationships: biochemistry versus genetics. *Trends Genet.* **21**, 424–427 (2005).
17. Wong, S.L. *et al.* Combining biological networks to predict genetic interactions. *Proc. Natl. Acad. Sci. USA* **101**, 15682–15687 (2004).
18. Drees, B.L. *et al.* Derivation of genetic interaction networks from quantitative phenotype data. *Genome Biol.* **6**, R38 (2005).
19. Segre, D., Deluna, A., Church, G.M. & Kishony, R. Modular epistasis in yeast metabolism. *Nat. Genet.* **37**, 77–83 (2005).
20. Collins, S.R., Schuldiner, M., Krogan, N.J. & Weissman, J.S. A strategy for extracting and analyzing large-scale quantitative epistatic interaction data. *Genome Biol.* **7**, R63 (2006).
21. Lee, W. *et al.* Genome-wide requirements for resistance to functionally distinct DNA-damaging agents. *PLoS Genet.* **1**, e24 (2005).
22. Giaever, G. *et al.* Functional profiling of the *Saccharomyces cerevisiae* genome. *Nature* **418**, 387–391 (2002).
23. Ashburner, M. *et al.* Gene ontology: tool for the unification of biology. The Gene Ontology Consortium. *Nat. Genet.* **25**, 25–29 (2000).
24. Ye, P., Peyser, B.D., Spencer, F.A. & Bader, J.S. Commensurate distances and similar motifs in genetic congruence and protein interaction networks in yeast. *BMC Bioinformatics* **6**, 270 (2005).
25. Kaliraman, V., Mullen, J.R., Fricke, W.M., Bastin-Shanower, S.A. & Brill, S.J. Functional overlap between Sgs1-Top3 and the Mms4-Mus81 endonuclease. *Genes Dev.* **15**, 2730–2740 (2001).
26. Shor, E., Weinstein, J. & Rothstein, R. A genetic screen for top3 suppressors in *Saccharomyces cerevisiae* identifies SHU1, SHU2, PSY3 and CSM2: four genes involved in error-free DNA repair. *Genetics* **169**, 1275–1289 (2005).
27. Friedl, A.A., Liefshitz, B., Steinlauf, R. & Kupiec, M. Deletion of the SRS2 gene suppresses elevated recombination and DNA damage sensitivity in *rad5* and *rad18* mutants of *Saccharomyces cerevisiae*. *Mutat. Res.* **486**, 137–146 (2001).
28. Ulrich, H.D. & Jentsch, S. Two RING finger proteins mediate cooperation between ubiquitin-conjugating enzymes in DNA repair. *EMBO J.* **19**, 3388–3397 (2000).
29. Huang, M.E., Rio, A.G., Nicolas, A. & Kolodner, R.D. A genomewide screen in *Saccharomyces cerevisiae* for genes that suppress the accumulation of mutations. *Proc. Natl. Acad. Sci. USA* **100**, 11529–11534 (2003).
30. Punnett, R.C. *Mendelism* (Macmillan, New York, 1913).
31. Jana, S. Simulation of quantitative characters from qualitatively acting genes. I. Nonallelic gene interactions involving two or three loci. *Theor. Appl. Genet.* **42**, 119–124 (1972).
32. Ito, T. *et al.* A comprehensive two-hybrid analysis to explore the yeast protein interactome. *Proc. Natl. Acad. Sci. USA* **98**, 4569–4574 (2001).
33. Sung, P. Yeast Rad55 and Rad57 proteins form a heterodimer that functions with replication protein A to promote DNA strand exchange by Rad51 recombinase. *Genes Dev.* **11**, 1111–1121 (1997).
34. Avery, L. & Wasserman, S. Ordering gene function: the interpretation of epistasis in regulatory hierarchies. *Trends Genet.* **8**, 312–316 (1992).
35. Krogh, B.O. & Symington, L.S. Recombination proteins in yeast. *Annu. Rev. Genet.* **38**, 233–271 (2004).
36. Lisby, M., Barlow, J.H., Burgess, R.C. & Rothstein, R. Choreography of the DNA damage response: spatiotemporal relationships among checkpoint and repair proteins. *Cell* **118**, 699–713 (2004).
37. Ellis, N.A. *et al.* The Bloom's syndrome gene product is homologous to RecQ helicases. *Cell* **83**, 655–666 (1995).
38. Fabre, F., Chan, A., Heyer, W.D. & Gangloff, S. Alternate pathways involving Sgs1/Top3, Mus81/Mms4, and Srs2 prevent formation of toxic recombination intermediates from single-stranded gaps created by DNA replication. *Proc. Natl. Acad. Sci. USA* **99**, 16887–16892 (2002).
39. Liberi, G. *et al.* Rad51-dependent DNA structures accumulate at damaged replication forks in *sgs1* mutants defective in the yeast ortholog of BLM RecQ helicase. *Genes Dev.* **19**, 339–350 (2005).
40. Prakash, R. *et al. Saccharomyces cerevisiae MPH1* gene, required for homologous recombination-mediated mutation avoidance, encodes a 3′ to 5′ DNA helicase. *J. Biol. Chem.* **280**, 7854–7860 (2005).
41. Schurer, K.A., Rudolph, C., Ulrich, H.D. & Kramer, W. Yeast MPH1 gene functions in an error-free DNA damage bypass pathway that requires genes from Homologous recombination, but not from postreplicative repair. *Genetics* **166**, 1673–1686 (2004).
42. Meetei, A.R. *et al.* A human ortholog of archaeal DNA repair protein Hef is defective in Fanconi anemia complementation group M. *Nat. Genet.* **37**, 958–963 (2005).
43. Bai, Y. & Symington, L.S.A. Rad52 homolog is required for RAD51-independent mitotic recombination in *Saccharomyces cerevisiae*. *Genes Dev.* **10**, 2025–2037 (1996).
44. Klein, H.L. Mutations in recombinational repair and in checkpoint control genes suppress the lethal combination of *srs2Δ* with other DNA repair genes in *Saccharomyces cerevisiae*. *Genetics* **157**, 557–565 (2001).
45. McEachern, M.J. & Haber, J.E. Break-induced replication and recombinational telomere elongation in yeast. *Annu. Rev. Biochem.* **75**, 111–135 (2006).
46. Winzeler, E.A. *et al.* Functional characterization of the *S. cerevisiae* genome by gene deletion and parallel analysis. *Science* **285**, 901–906 (1999).
47. Guthrie, C. & Fink, G.R. (eds.) *Guide to Yeast Genetics and Molecular Biology* (Academic Press, New York, 1991).
48. Rose, M.D., Winston, F. & Heiter, P. *Methods in Yeast Genetics: a Laboratory Manual* (Cold Spring Harbor Laboratory Press, Cold Spring Harbor, New York, USA, 1990).
49. Erdeniz, N., Mortensen, U.H. & Rothstein, R. Cloning-free PCR-based allele replacement methods. *Genome Res.* **7**, 1174–1183 (1997).